Ultralow-angle dynamic light scattering with a charge coupled device camera based multispeckle, multitau correlator

Luca Cipelletti and D. A. Weitz
Department of Physics and Astronomy, University of Pennsylvania, Philadelphia, Pennsylvania 19104

(Received 18 December 1998; accepted for publication 11 May 1999)

We use a charge coupled device (CCD) camera and a multi-tau software correlator to measure dynamic light scattering (DLS) at many angles simultaneously, from 0.07° to 5.1°. Real-time autocorrelation functions are calculated by averaging both over time and over CCD pixels, each corresponding to a different coherence area. In order to cover the wide spectrum of decay times associated with the large range of accessible angles, we adopt the multitau scheme, where the correlator channel spacing is quasilogarithmic rather than linear. A detailed analysis is presented of the effects of dark noise, stray light, and finite pixel area, and methods to correct the data for these effects are developed, making a CCD camera a viable alternative for a DLS detector. We test the apparatus on a dilute suspension of colloidal particles. Very good agreement is found between the particle radius derived from the CCD data, and that obtained with a conventional DLS setup. [S0034-6748(99)05008-X]

I. INTRODUCTION

Dynamic light scattering (DLS) is a well-established technique for investigating the dynamics of a wide variety of systems. It has been successfully applied to countless problems in physics, chemistry, biology, and medicine. In a DLS experiment, the quantity of interest is the ensemble-averaged temporal autocorrelation function of the fluctuations of the light scattered by the sample. A typical setup includes a laser source, a goniometer, and a detector, usually a photomultiplier tube, whose signal is fed to an electronic correlator. The detector collects light from a single coherence area or speckle.[1,2] To obtain good statistical accuracy, it is necessary to extensively time-average the correlator output; for example, to attain a statistical uncertainty of 1% requires a measurement over 10 000 characteristic decay times of the correlation function. For ergodic samples, the time averaging directly yields the desired ensemble average. However, this approach may be difficult or even impossible for studying samples that are nonergodic, where time and ensemble averaging are no longer equivalent. This approach is also impractical for systems with very slow dynamics, where the averaging time becomes too long. Examples of systems of great interest which exhibit slow dynamics or nonergodic behavior include colloidal glasses and polymeric or colloidal gels. In addition, the interesting dynamics often occurs at length scales as large as several microns, corresponding to very small angles, and very slow dynamics. To measure DLS under these conditions requires a new strategy.

The most direct and effective approach is to use a multielement sensor, such as the pixel array of a charge coupled device (CCD) camera, to collect the signal from many different speckles simultaneously. For slow dynamics, correlation functions can be calculated by software for each pixel and then averaged. Since different speckles are statistically independent, the pixel averaging enhances the statistical accuracy and the total duration of the experiment can be reduced by a factor equal to the number of coherence areas sampled. Under proper conditions, direct ensemble averaging is also possible, thus allowing one to study nonergodic samples. Wong and Wiltzius[3] first demonstrated the feasibility of this approach by measuring DLS with a CCD camera. Autocorrelation functions were averaged over rings of pixels centered about the transmitted beam position, that is, over speckles corresponding to the same magnitude of the scattering wave vector $q \equiv |\mathbf{q}|$ but different azimuthal orientation, where $q = 4\pi\lambda^{-1} \sin\theta/2$, θ is the scattering angle, and λ is the wavelength in the medium. This geometry was also used to help overcome the very low scattered intensity encountered in the extension of speckle correlation spectroscopy to small-angle x rays.[5–7] So-called ''multispeckle'' autocorrelation functions were also measured by Kirsch *et al.*,[4] who incorporated a CCD detector in a traditional DLS setup. In their case, the averaging was not azimuthal, but rather over a limited number of speckles corresponding to a small solid angle centered around the direction set by the goniometer arm.

Despite the increasing use of CCD cameras for correlation spectroscopies, many important issues have not, as yet, been addressed. The algorithms used cannot meet the computational load required to calculate in real time the autocorrelation functions averaged over both pixels and time. The constrains and limitations specific to a CCD sensor have not been fully addressed. Due to the reduced dynamic range (typically 2–3 decades), the contribution of the dark noise to the autocorrelation function can be significant, as can the distortions introduced by pixel saturation. Moreover, the finite pixel-to-speckle size ratio must be taken into account to obtain the absolute scale of the autocorrelation functions. These limitations have restricted the use of CCD cameras to samples for which the shape of the autocorrelation function was known *a priori*,[3,5–7] or to samples where some overlap existed with data obtained with a traditional setup.[4] For light

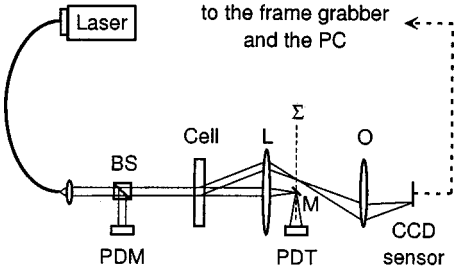

FIG. 1. Experimental setup.

scattering, CCD cameras are particularly well suited for ultrasmall-angle scattering, where the speckle averaging and the capability of collecting data at many scattering angles simultaneously match well with the wide range of azimuthal and scattering angles usually accessible in a low-q apparatus. The relatively low data acquisition rate of a CCD camera is of little concern, since at small q the speckle dynamics are slow. However, at small angles, stray light scattered from the optical components can often dominate the total intensity; while this can be subtracted from the average or static intensity, it can mix with the fluctuations, leading to severe distortions of the correlation function. Thus, special care must be taken to correct for these effects.

In this article, we discuss the implementation of an apparatus for measuring DLS at ultrasmall angles using a CCD camera. We access angles from 0.07° to 5.1°, corresponding to length scales spanning almost two decades, from a few microns to a fraction of a millimeter. To simultaneously cover the wide spectrum of relaxation times associated with such a large range of length scales, we adopt the multitau correlation scheme,[9] where the delay times are spaced quasi-logarithmically, rather than linearly. The multitau algorithm requires less data storage and processing time, thus allowing us to calculate time- and pixel-averaged autocorrelation functions in real time. Multiple exposure times are also used, to optimize the mean intensity level for all scattering vectors. A detailed analysis of the effects of dark noise, stray light, and finite detector area on the autocorrelation function is presented. Formulas are derived that allow us to extract the field autocorrelation function from the measured CCD signal autocorrelation. The correlator algorithm and the data correction procedure are designed to study both ergodic and nonergodic samples.

In Sec. II of this article, we describe the experimental setup, while in Sec. III, we present our implementation of the software multitau, multispeckle correlator, focusing first on the algorithm (Sec. III A), then on the corrections needed to account for stray light, dark noise and pixel area (Sec. III B). Finally, in Sec. IV we describe and discuss an experimental test of the apparatus.

II. EXPERIMENTAL SETUP

The experimental setup is shown in Fig. 1. The light source is a frequency-doubled Nd:YAG laser (Coherent 315M) that operates at a wavelength of 532 nm. The laser beam is coupled to a polarization-maintaining single-mode fiber optics. We use a set screw to partially block the beam before coupling it to the fiber, so that the beam power can be attenuated to a few μW, as required for a typical measurement. The beam exiting the fiber is collimated by a lens to a $1/e^2$ diameter of 7.7 mm and a portion is directed by a beam splitter (BS) onto a photodiode (PDM), which monitors any fluctuations in the incident power. The transmitted component impinges onto the scattering cell, which is typically a flat cell, 2–10 mm in thickness. The optical scheme for the collection of the scattered light is similar to that described by Ferri.[8] Both the scattered and the transmitted light are collected by a lens (L) with a focal length of 100 mm. In its focal plane Σ, a small mirror (M) is placed, at an angle of 45° to the incident beam. The transmitted beam is intercepted by this mirror and directed to a photodiode (PDT), allowing the sample transmission to be measured. The CCD objective (O) images the focal plane Σ onto the CCD sensor with unit magnification. With this optical scheme, each CCD pixel corresponds to a different scattering wave vector $\mathbf{q}$. Scattering wave vectors of the same magnitude q are mapped to pixels lying on a circle centered about the optical axis. The optics are designed in such a way that the speckle size in the sensor plane corresponds roughly to the pixel size. Almost two decades in scattering vector are accessible: $200\,\mathrm{cm}^{-1} \leqslant q \leqslant 14\,000\,\mathrm{cm}^{-1}$, corresponding to scattering angles from about 0.07° to 5.1°. The minimum angle is limited by the size of the small mirror that blocks the transmitted beam, while the angular range is dictated by the sensor size. The CCD camera is a 10-bit digital camera (Eastman Kodak Megaplus 1.6i) with a 1532×1024 pixel sensor, each pixel being 9×9 $\mu\mathrm{m}^2$. The maximum camera speed is 5 frames per second. The digitized images are acquired by a frame grabber (Matrox Pulsar) and transferred for real-time processing to a PC with an Intel Pentium II processor running at 400 MHz.

III. SOFTWARE CORRELATOR

We outline the general features of the multitau, multispeckle algorithm in Sec. III A. The effects on the measured autocorrelation functions of the CCD dark noise, stray light, the finite pixel-to-speckle size ratio are discussed in Sec. III B. Formulas are derived to correct for the distortions due to these effects.

A. Multitau, multispeckle autocorrelation function calculation

We use custom-written software to calculate real-time autocorrelation functions in parallel for all pixels processed. To access a wide range of delay times without exceeding the PC memory and computation power, the multitau correlator scheme first proposed by Schätzel[9] is adopted. In order to obtain good statistics even for short runs and to study nonergodic samples, the autocorrelation functions calculated for all pixels with the same magnitude of the scattering vector are averaged. Let us first focus on the calculation of the autocorrelation function for a single pixel. In the multitau scheme, the correlator channel spacing is quasi-logarithmic, thus spanning several decades in delay times with a limited number of channels. The algorithm consists of implementing

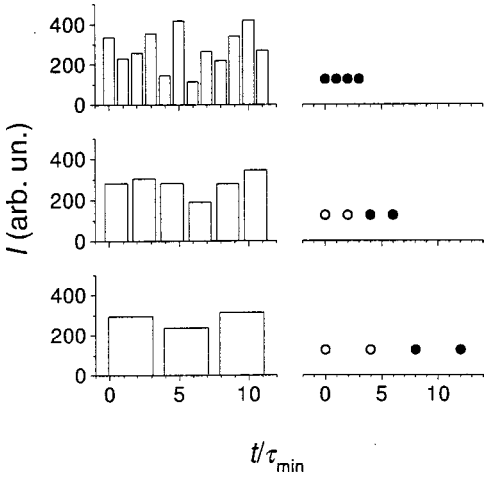

FIG. 2. Schematic sketch of the multi-tau correlator architecture. The streams of data input to the linear correlators are plotted on the left, from the fastest (top) to the slowest (bottom). The width of the columns is proportional to the sampling time. The channel spacing for each linear correlator is shown on the right. Only channels represented by the filled symbols are actually processed. For clarity, only three linear correlators with four channels each are shown.

a set of linear correlators, each of which has a small number of channels, typically sixteen, evenly spaced in time. The delay time is not the same for all correlators, but rather doubles from one correlator to the next. To increase the statistical accuracy, the sampling time also doubles with the delay time, as shown schematically in Fig. 2. The desired multitau autocorrelation function is obtained by merging the output of all linear correlators. Note that for all correlators but the first, the autocorrelation function needs to be calculated only for the second half of the channels, since the first half corresponds to time delays already covered by the faster correlators. The input for the first correlator is the data from the CCD camera, whose frame rate and exposure time set the shortest delay time $\tau_{\min}$ and sampling time $\tau_{\exp}$, respectively. Pairs of subsequent data are then combined by averaging them, and input into the next correlator. This scheme is iterated for all linear correlators. The averaging process deserves a brief comment. To reduce the amount of required memory, the smallest data format that can accommodate the 10-bit CCD data, 16-bit integers, is adopted for all correlators. Because of this integer format, whenever the sum of the two data points to be combined is odd, the average is underestimated by 0.5 intensity levels (or counts), due to the round-off inherent in integer division. This would result in a spurious ''jump'' in the multitau autocorrelation function when changing from a set of channels at a given time delay separation to the next set. We avoid this artifact by randomly adding 1, with probability $\frac{1}{2}$, to the sum of the pair of data, prior to division. Thus, the data fed to the slower linear correlators are equally likely to be (slightly) underestimated or overestimated, and on average the round-off errors cancel.

We now describe the averaging of the multitau autocorrelation functions calculated for different pixels, and therefore speckles, but for the same magnitude q of the scattering vector. The un-normalized intensity autocorrelation function $G_I(q,\tau)$ is calculated by averaging over the appropriate set of pixels:

$$G_I(q,\tau)=\langle\langle I_p(t)I_p(t+\tau)\rangle_\phi\rangle_t, \tag{1}$$

where $I_p(t)$ is the pth pixel intensity at time t, and $\langle\ldots\rangle_\phi$ and $\langle\ldots\rangle_t$ indicate the azimuthal averaging over all pixels associated to the same q and the time average, respectively. The normalized intensity autocorrelation function $g_I(q,\tau)$ is computed by applying a ''fully symmetric'' normalization scheme:

$$g_I(q,\tau)=G_I(q,\tau)/[\langle\langle I_p(t)\rangle_\phi\rangle_{0\le t\le t_{\rm run}-\tau}\langle\langle I_p(t)\rangle_\phi\rangle_{\tau\le t\le t_{\rm run}}], \tag{2}$$

where $t_{\rm run}$ is the duration of the experiment, and $\langle\ldots\rangle_{t_1\le t\le t_2}$ indicates the time averaging from time t_1 to time t_2, the measurement being started at time $t=0$. The normalization in Eq. (2) reduces the sensitivity to drifts in laser power, an essential feature when running long measurements and when the largest delay time becomes comparable to the duration of the experiment. This reduced sensitivity is obtained by averaging the values of the mean intensity that appear in the denominator of Eq. (2) over the same periods of time during which the data used to calculate $G_I(q,\tau)$ are collected. It is important to notice that the autocorrelation function is first averaged over all pixels and then normalized. For an ergodic sample, one could equivalently follow the reverse order, i.e., average the normalized, time-averaged autocorrelation functions calculated for each individual pixel. However, this would be computationally less efficient, since one would need to keep in the computer memory a very large number of correlation functions (one per processed pixel, instead of one for each q). More importantly, this order is essential for a nonergodic system, since it directly yields the ensemble-averaged autocorrelation function.[10,11] We emphasize, however, that in order to obtain the ensemble average by pixel averaging, the scattering volume must be large enough to be statistically representative of the whole sample; thus the sample must be homogeneous over length scales comparable to the incident beam width. As a consequence, the sample must be illuminated with a broad beam, as described in Sec. II. Finally, we note that there are similarities between the pixel-averaging method described above and other schemes proposed in the past for studying nonergodic samples with a single detector, where the contribution of different speckles to the autocorrelation function was obtained by rotating or translating the sample during the measurement.[12,13] However, the multispeckle technique has the significant advantage of collecting data in parallel rather than sequentially; thus for a given total measurement time, much longer time delays are accessible.

In a typical experiment, the calculation is carried out simultaneously for several sets of pixels, corresponding to different values of q. Given the wide range of accessible scattering vectors, the mean intensity may vary considerably from one set of pixels to the other. This poses a serious problem, due to the limited dynamic range of the CCD sensor. To overcome this limitation and to optimize the measured mean intensity at all scattering angles, for every $\tau_{\min}$

we collect a sequence of a few frames (typically 3–5), each at a different exposure time, instead of acquiring an image with a single exposure time. For each scattering angle, only the data at the most suitable exposure time are processed. Experimentally, we find that the optimal mean intensity is about 15% of the saturation level, corresponding to 150 counts for a 10-bit camera. Lower mean count values yield an appreciably poorer signal-to-noise ratio, while higher values cause a significant fraction of the CCD pixels to saturate.

B. Corrections for dark counts, stray light, and finite sensor area

In this subsection, we describe how the measured autocorrelation functions are corrected for the effects of dark counts, stray light, and finite sensor area to obtain the desired physical quantity, the normalized field autocorrelation function

$$g_E(q,\tau)=\langle E_p(t)E_p^*(t+\tau)\rangle_{\phi,t}/\langle I_p(t)\rangle_{\phi,t}, \tag{3}$$

where $\langle\ldots\rangle_{\phi,t}$ denotes the average first over pixels and then over time. The correction scheme proposed here is also applicable to nonergodic samples, since it is based on an independent measurement of the contribution of stray light to the total scattering, with no assumptions being made about the full decay of the correlation function. Before describing the details of the correction procedure, we briefly discuss the physical origin and the importance of each of these effects. Dark counts are due to thermal and pixel read-out noise, as well as to an offset in the setting of the black-level reference voltage of the digitizer. They can be a significant fraction of the measured intensity level because of the limited dynamic range of the CCD, and consequently they can appreciably distort the measured autocorrelation function. In particular, the presence of a constant offset is reflected in a spurious correlation at long time delays. The stray light is due to scattering from the optical components themselves (lenses and cell walls) and is therefore a static contribution. Its impact can be reduced by using carefully cleaned, high-quality optical elements and by disregarding pixels that are obviously saturated due to flare and backreflections. However, stray light is unavoidable at low angles, where its intensity can be equal to or even larger than the scattering from the sample alone. Stray light acts as a local oscillator,[1] mixing with the field scattered by the sample. Therefore, the DLS signal is no longer purely homodyne. The effect of some degree of heterodyning is twofold. First, the autocorrelation function base line is raised, since the static stray light gives a finite contribution at any delay time. Second, the decay rate is changed. Note that the amount of mixing, i.e., the intensity of the stray light, is constant in time but varies from pixel to pixel. The effect of the finite pixel area, compared to the speckle area, is to decrease the amplitude of the time-varying part of the intensity autocorrelation function $G_I(q,\tau)$. Under homodyne conditions, this reduction is accounted for by a multiplicative constant, the so-called coherence factor β_I.[1] The generalization to the case of a heterodyne signal will be discussed at the end of this section.

We will now derive an expression that relates the field autocorrelation function for the light scattered by the sample alone to the measured intensity autocorrelation function. We first consider the simpler but rather uncommon case where the pixel size is much smaller than the speckle size, so that $\beta_I=1$. The intensity on the CCD at time t and pixel p is

$$S_p(t)=D_p(t)+[E_p(t)+E_{sl,p}][E_p^*(t)+E_{sl,p}^*], \tag{4}$$

where $D_p(t)$ is the dark count level, $E_p(t)$ is the field scattered by the sample, $E_{sl,p}$ is the pixel-dependent stray light field which is constant in time, and all nonessential multiplicative constants have been dropped. The autocorrelation function that is experimentally measured is

$$G_S(q,\tau)=\langle S_p(t)S_p(t+\tau)\rangle_{\phi,t}. \tag{5}$$

By using Eq. (4), $G_S(q,\tau)$ can be expressed in terms of the dark counts and the scattered light

$$\begin{aligned}G_S(q,\tau)=&G_I(q,\tau)+\langle I_{sl}^2\rangle_{\phi,t}+2\langle I_{sl}\rangle_{\phi,t}\langle I\rangle_{\phi,t}\\&+2\langle D\rangle_{\phi,t}[\langle I_{sl}\rangle_{\phi,t}+\langle I\rangle_{\phi,t}]\\&+2\langle I_{sl}\rangle_{\phi,t}G_E(q,\tau)+G_D(q,\tau).\end{aligned} \tag{6}$$

In Eq. (6), I and I_{sl} are the scattering intensity from the sample and the stray light, respectively; $G_D(q,\tau)$ is the autocorrelation function of dark counts, and $G_E(q,\tau)$ is the field autocorrelation from the sample, which is the quantity we wish to determine. For brevity, here and in the following the explicit dependence on time and pixels has been omitted. In deriving Eq. (6), we have made the following assumptions:

(i) Both E and E_{sl} obey the statistics of speckle fields, thus they are stationary, zero-mean circular complex Gaussian random variables. It follows that $\langle E\rangle_\phi=\langle E_{sl}\rangle_\phi=0$ and $\langle I\rangle_\phi=\text{const}$ and $\langle I_{sl}\rangle_\phi=\text{const}$.

(ii) E and E_{sl} are uncorrelated, so that $\langle EE_{sl}^*\rangle_\phi=\langle E\rangle_\phi\langle E_{sl}^*\rangle_\phi=0$.

(iii) The dark count level, the stray light, and the scattered intensity are mutually uncorrelated, so that $\langle ID\rangle_\phi=\langle I\rangle_\phi\langle D\rangle_\phi$, $\langle I_{sl}D\rangle_\phi=\langle I_{sl}\rangle_\phi\langle D\rangle_\phi$, and $\langle I_{sl}I\rangle_\phi=\langle I_{sl}\rangle_\phi\langle I\rangle_\phi$.

Equation (6) is the first step for expressing the field autocorrelation function in terms of measurable quantities. To proceed further, we make use of the Siegert relation[1,2]

$$G_I(q,\tau)=\langle I\rangle_{\phi,t}^2+[G_E(q,\tau)]^2. \tag{7}$$

Insertion of the Siegert relation in Eq. (6) yields

$$\begin{aligned}&[G_E(q,\tau)]^2+2\langle I_{sl}\rangle_{\phi,t}G_E(q,\tau)+\langle I_{sl}^2\rangle_{\phi,t}+\langle I\rangle_{\phi,t}^2\\&+2\langle I_{sl}\rangle_{\phi,t}\langle I\rangle_{\phi,t}+2\langle D\rangle_{\phi,t}[\langle I_{sl}\rangle_{\phi,t}+\langle I\rangle_{\phi,t}]\\&+G_D(q,\tau)-G_S(q,\tau)=0.\end{aligned} \tag{8}$$

$G_E(q,\tau)$ can be obtained by solving Eq. (8), since all other quantities are experimentally accessible, as we will now show. We start with the quantities related to the dark noise. Test measurements show that, although the dark noise for a

single pixel is time dependent, its azimuthal average $\langle D\rangle_\phi$ is constant. Moreover, the dark noise is found to be uncorrelated. Therefore,

$$G_D(q,\tau)=\begin{cases}\langle D^2\rangle_{\phi,t}, & \tau=0\\ \langle D\rangle^2_{\phi,t}, & \tau\neq 0\end{cases} \tag{9}$$

and $\langle D\rangle_{\phi,t}$ and $\langle D^2\rangle_{\phi,t}$ can be easily measured by acquiring a set of frames with the CCD shutter closed. Similarly, the stray light contribution can be measured prior to the run by filling the cell with just the solvent. This procedure is routinely adopted in very small angle static light scattering measurements.[8] We tested its applicability to DLS by measuring the autocorrelation function of the stray light alone. No appreciable time dependence was found, thus demonstrating that $E_{sl,p}$ is constant in time and that stray light can be reliably measured by this procedure. Finally, the mean scattering from the sample alone can be obtained by subtracting the stray light from the measured total scattered intensity. In subtracting the stray light, care must be taken to normalize it by the sample transmission T, since the stray light will be attenuated by a factor T due to the presence of the scattering sample.[8] We measure T by comparing the signal at the transmitted-beam photodiode in the presence of the sample to that when the cell is filled with the solvent alone. Note that the cell cannot be moved after measuring the optical background, to avoid changes in the stray light. To summarize, $\langle I\rangle_{\phi,t}$, $\langle I_{sl}\rangle_{\phi,t}$, and $\langle I^2_{sl}\rangle_{\phi,t}$ are obtained from

$$\langle I_{sl}\rangle_{\phi,t}=T[\langle S_{sl}\rangle_{\phi,t}-\langle D\rangle_{\phi,t}], \tag{10a}$$

$$\langle I^2_{sl}\rangle_{\phi,t}=T^2\{\langle S^2_{sl}\rangle_{\phi,t}-2\langle D\rangle_{\phi,t}[\langle S_{sl}\rangle_{\phi,t}-\langle D\rangle_{\phi,t}]-\langle D^2\rangle_{\phi,t}\}, \tag{10b}$$

$$\langle I\rangle_{\phi,t}=\langle S\rangle_{\phi,t}-\langle D\rangle_{\phi,t}-\langle I_{sl}\rangle_{\phi,t}, \tag{10c}$$

where S_{sl} is the CCD signal when the cell is filled just with the solvent. We have thus shown that Eq. (8) together with Eqs. (9) and (10) allows one to calculate the field autocorrelation function $G_E(q,\tau)$ from measurable quantities: the measured autocorrelation function, $G_S(q,\tau)$, the total scattering, and the dark noise and stray light. Normalizing $G_E(q,\tau)$ by $\langle I\rangle_{\phi,t}$ yields $g_E(q,\tau)$, the normalized field autocorrelation function.

So far we have assumed that the pixel size is negligible compared to the speckle size. More generally, we must extend the above relations to the more common case of a finite sensor size, where the pixel and speckle sizes are comparable. This can be done by replacing Eq. (4) by

$$S_p(t)=D_p(t)+\int_{A_p} d^2\mathbf{x}[I(\mathbf{x},t)+I_{sl}(\mathbf{x}) + E(\mathbf{x},t)E^*_{sl}(\mathbf{x})+E^*(\mathbf{x},t)E_{sl}(\mathbf{x})], \tag{11}$$

where the integration is over the pixel area A_p and where we have explicitly included the spatial dependence of the scattered and stray-light fields (again, inessential multiplicative constants have been dropped). By interchanging the order of integration and averaging, it is easy to show that the mean value of the intensity is not affected by the pixel integration. Then, the only terms that need to be modified in Eq. (6) are $G_I(q,\tau)$, $\langle I^2_{sl}\rangle_{\phi,t}$, and $2\langle I_{sl}\rangle_{\phi,t}G_E(q,\tau)$. The first term can be expanded by means of the modified Siegert relation:[1,2]

$$G_I(q,\tau)=\langle I\rangle^2_{\phi,t}+\beta_I[G_E(q,\tau)]^2. \tag{12}$$

This is the familiar correction introduced in a homodyne experiment to account for the finite sensor area. The coherence factor β_I can be calculated from the detector geometry and the beam intensity profile:

$$\beta_I=\int d^2\mathbf{x}R_A(\mathbf{x})|\mu(\mathbf{x})|^2, \tag{13}$$

where the so-called complex coherent factor $\mu(\mathbf{x})$ is the normalized Fourier transform of the beam intensity profile, while $R_A(\mathbf{x})$ is simply related to the detector geometry.[2] The second term, $\langle I^2_{sl}\rangle_{\phi,t}$, could be expanded in a similar way. However, this is unnecessary since $\langle I^2_{sl}\rangle_{\phi,t}$ can be obtained directly from measured quantities through Eqs. (10). Due to integration over the pixel area, the last term, $2\langle I_{sl}\rangle_{\phi,t}G_E(q,\tau)$, is reduced by a factor β^2_E, where

$$\beta_E=\int d^2\mathbf{x}R_A(\mathbf{x})\mu(\mathbf{x}). \tag{14}$$

A factor of β_E arises from the spatial integration of the cross term $\langle E(\mathbf{x}_1,t)E^*(\mathbf{x}_2,t+\tau)\rangle_{\phi,t}$.[14] An additional factor of β_E arises from the analogous integration of the spatially fluctuating stray light cross term $\langle E_{sl}(\mathbf{x}_1)E^*_{sl}(\mathbf{x}_2)\rangle_{\phi,t}$. If the pixel area is negligible, this term reduces to the $\langle I_{sl}\rangle_{\phi,t}$ factor in Eq. (6).

We can now generalize Eq. (8) to the more realistic case of a finite pixel size:

$$\beta_I[G_E(q,\tau)]^2+2\beta^2_E\langle I_{sl}\rangle_{\phi,t}G_E(q,\tau)+\langle I^2_{sl}\rangle_{\phi,t}+\langle I\rangle^2_{\phi,t} + 2\langle I_{sl}\rangle_{\phi,t}\langle I\rangle_{\phi,t}+2\langle D\rangle_{\phi,t}[\langle I_{sl}\rangle_{\phi,t}+\langle I\rangle_{\phi,t}] + G_D(q,\tau)-G_S(q,\tau)=0. \tag{15}$$

This equation is the main theoretical result of this article. Together with Eqs. (9) and (10), it constitutes the desired formula for correcting DLS data from a CCD camera for the effects of dark noise, stray light, and finite pixel area. It can be solved for $G_E(q,\tau)$; the normalized field autocorrelation function is then obtained as before from $g_E(q,\tau)=G_E(q,\tau)/\langle I\rangle_{\phi,t}$. In order to apply Eq. (15), it is necessary to evaluate β_I and β_E. Although it is possible to calculate them from the beam $1/e^2$ diameter and the pixel size,[2] we rather derive their value from the intensity autocorrelation measured at $\tau=0$. In fact, by definition $G_E(q,0)=\langle I\rangle_{\phi,t}$, so that for $\tau=0$ the only unknowns in Eq. (15) are β_I and β_E. Moreover, from the theoretical expression of the complex coherence factor μ, we can calculate β^2_E as a function of β_I. We find that, for the experimental parameters of our setup, $\beta^2_E\approx\beta_I\approx 0.55$ and that the following linear approximation may be used

$$\beta^2_E=-0.14+1.18\beta_I. \tag{16}$$

Operationally, we thus insert Eq. (16) in Eq. (15) evaluated at $\tau=0$, and solve for β_I.

This correction scheme is also applicable to nonergodic samples, provided the required values for the stray light and the dark counts can be obtained from a measurement of the cell filled with the solvent alone. The question is then whether or not assumptions (i–iii) made in deriving the correction formula still hold for a nonergodic sample, thus we must determine if $\langle E\rangle_\phi = 0$, $\langle EE_{sl}^*\rangle_\phi = 0$, and $\langle ID\rangle_\phi = \langle I\rangle_\phi\langle D\rangle_\phi$. For a nonergodic sample, the scattered field can be decomposed to a sum of a constant and a time-varying part.[10] If there is a constant component, the *temporal* statistical properties of E and EE_{sl}^* change; thus the scattered field is no longer zero mean and it is partially correlated to the static stray light field. However, its spatial statistical properties are unaffected. Since assumptions (i) and (ii) involve only spatial averaging, they can be safely assumed to be also valid for a nonergodic sample. Similarly, the coherence factors β_I and β_E are calculated from the value of $G_S(q,\tau=0)$, which is averaged first spatially and then temporally, and therefore their values do not depend on the sample ergodicity. This is in contrast with the case of a traditional setup, for which β_I is derived from a purely temporal average, and thus can largely vary for nonergodic samples.[10] Finally, assumption (iii) is clearly independent of the nature of the sample. Therefore, we conclude that the correction procedure is valid for all samples both ergodic and nonergodic. We emphasize, however, that if the time averaging is carried out before the pixel averaging, then this argument does not hold and the correction scheme would fail when applied to nonergodic samples.

IV. EXPERIMENTAL TEST AND DISCUSSION

We have experimentally tested the apparatus by measuring the autocorrelation function of the light scattered by a diluted suspension of polystyrene spheres. The spheres (Seradyn lot JS 2678) had a radius of 1.095 μm and a polidispersity of about 5%, as rated by the manufacturer, and were suspended at a volume fraction $\varphi \approx 3\times10^{-5}$. To avoid sedimentation, we used a buoyancy-matching mixture of H_2O and D_2O as a solvent. Note that, unlike the case of a traditional DLS experiment, sedimentation does contribute to the decay of the correlation functions for the CCD-based apparatus; this is due to the average over different orientations of **q** and to the heterodyning induced by stray light. The experiment was done at room temperature (22 ± 1 °C). Autocorrelation functions for twelve different scattering vectors ranging from $q = 302\,\mathrm{cm}^{-1}$ to $q = 12\,412\,\mathrm{cm}^{-1}$ were simultaneously measured. The run duration was 2560 s, the minimum time delay $\tau_{\min}$ being 1.25 s. For each q, the autocorrelation function was azimuthally averaged over a ring of pixels centered about the optical axis and over time, following the procedure described above. The mean radius and the thickness of these rings were chosen to increase with the same power law, keeping their ratio (approximately) constant, and evenly spacing the values of q on a logarithmic scale. The total number of processed pixels was 115 499, limited primarily by the computer speed. Three different exposure times were used to optimize the mean intensity level at all q vectors, as explained in Sec. III A. To apply the stray light correction described above, the cell was filled with the solvent alone and the stray light intensity was measured prior to the DLS runs. We used a pipette to remove the solvent and to insert the particle suspension without moving the cell from its holder, thus avoiding any changes in the stray light due to a change in the cell position. Table I lists the principal measurement parameters.

TABLE I. Measurement parameters for the experimental test of the apparatus. For each scattering vector q, we report the relative uncertainty $\delta q/q$ (due to the thickness of the ring of pixels associated to q), the exposure time $\tau_{\exp}$, the number of processed pixels N_q, and the ratio between the mean stray light intensity and the mean intensity of the light scattered by the sample alone, $\langle I_{sl}\rangle_{\phi,t}/\langle I\rangle_{\phi,t}$.

q (cm^{-1})	$\delta q/q$	$\tau_{\exp}$ (ms)	N_q	$\langle I_{sl}\rangle_{\phi,t}/\langle I\rangle_{\phi,t}$
302	3.4×10^{-2}	20	87	6.937
428	2.4×10^{-2}	20	183	2.490
594	1.8×10^{-2}	20	281	2.159
834	2.5×10^{-2}	20	865	1.226
1158	3.4×10^{-2}	49	1902	0.722
1627	2.7×10^{-2}	49	3616	0.266
2273	2.6×10^{-2}	49	4855	0.091
3191	2.3×10^{-2}	49	8579	0.043
4461	2.3×10^{-2}	49	16015	0.025
6240	2.5×10^{-2}	49	24584	0.021
8730	2.5×10^{-2}	49	41467	0.022
12412	2.5×10^{-2}	120	13065	0.025

In Fig. 3 we show on a semilogarithmic plot a typical set of measured normalized intensity autocorrelation functions. Here the autocorrelation functions are corrected only for the contribution of the dark noise. Figure 3(a) shows the autocorrelation functions for the six largest q, while Fig. 3(b) shows the data taken at the lowest angles (note the difference in the x axis scale). Very good quality data are obtained even at the lowest angles, for which the run duration is just a few times the autocorrelation function decay time, due to the averaging over pixels. At higher angles, the autocorrelation functions decay exponentially for about two decades, as evidenced by the linear behavior on the semilogarithmic plot. This behavior is expected for a dilute suspension of spheres undergoing brownian motion.[1] At lower angles, the autocorrelation functions do not decay completely, reaching a plateau at long time delays τ. The plateau is due to the static

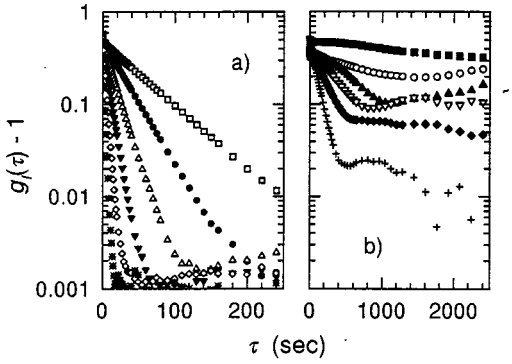

FIG. 3. Intensity autocorrelation functions simultaneously measured at twelve scattering vectors. From top to bottom: (a) 2273, 3191, 4461, 6240, 8730, and 12 412 cm^{-1}; (b) 302, 428, 594, 834, 1158, and 1627 cm^{-1}. The data are corrected only for the CCD dark noise.

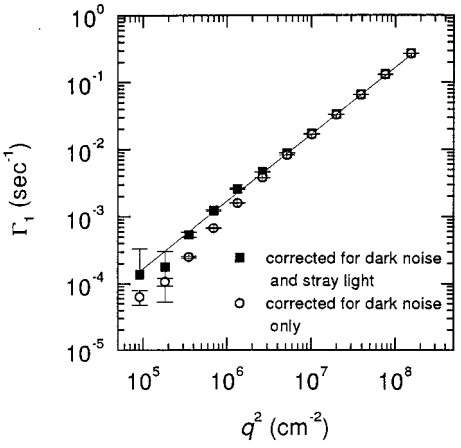

FIG. 4. Decay rate Γ_1, averaged over five runs, from a second-order cumulant fit of the measured autocorrelation functions. Open circles refer to the data corrected only for the CCD dark noise, filled squares to the data corrected for both dark noise and stray light.

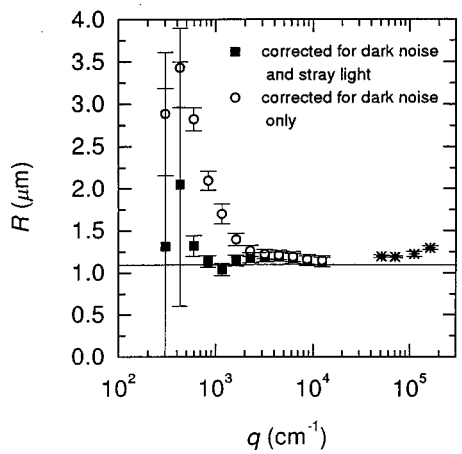

FIG. 5. Particle radius R calculated by means of the Stokes–Einstein relationship from the decay rates shown in Fig. 4 (open circles and filled squares). The stars are values of R obtained with a traditional setup and a hardware correlator at 18°, 25°, 45°, and 60°. The line is the manufacturer's value for R.

contribution of the stray light, which prevents the scattered intensity from being completely decorrelated even at very large τ. The height of the plateau increases with decreasing scattering vector, reflecting the increase, at lower angles, of the stray light intensity compared to the scattering from the sample alone (see Table I). The noise observed at long time delays and small q is due to long-term power fluctuations of the incident beam, and to the poorer statistics of the autocorrelation functions at the smaller angles. In fact, both the number of pixels per ring and the number of decorrelation times (the physically relevant time scale) decrease with q. Thus, a reduced number of statistically independent data contribute to the pixel and time average. Finally, the intercepts at $\tau=0$ of the autocorrelation functions are lower than 1, due to the finite pixel size, and change slightly with q, due to saturation effects that depend on the value of the mean intensity.[15] The angular dependence of the intercept is minimized by optimizing the exposure time for each q, as described before.

To obtain quantitative information from the autocorrelation functions, we perform a cumulant analysis,[1] fitting to the following expression:

$$\ln[g_E(q,\tau)]=\Gamma_0-\Gamma_1\tau-\frac{1}{2!}\Gamma_2\tau^2-\frac{1}{3!}\Gamma_3\tau^3-\cdots \quad (17)$$

Figure 4 shows a log-log plot of the decay rate Γ_1, obtained from an average over five runs, as a function of q^2. We obtained Γ_1 from a second-order cumulant analysis of the autocorrelations functions, corrected for the dark noise only (open circles) and for both the dark noise and the stray light (filled squares). A first-order cumulant analysis yielded similar results, the fit being less good due to the slightly polidisperse sample and, for the uncorrected data (open circles), to the contribution of the stray light. The decay rates span more than three decades, due to the wide range of scattering vectors q. To simultaneously cover such a large spectrum of characteristic decorrelation times, the adoption of the multi-tau correlator scheme is mandatory. At larger angles, the two sets of data superimpose and Γ_1 is linear in q^2, in agreement with expectations for a purely diffusive system, for which $\Gamma_1=Dq^2$, where D is the particle diffusion coefficient. At lower angles, the data which are corrected only for dark noise deviate from the linear behavior, with Γ_1 being increasingly lower than expected. Qualitatively, this trend can be understood; due to the stray light, the signal is not measured under homodyne conditions, but rather under partial heterodyne conditions. The lower the angle, the stronger the stray light contribution and the closer the signal to purely heterodyne conditions, for which the decay rate is half of that measured in a homodyne experiment.[1] However, by correcting the autocorrelation functions for the stray light as described in Sec. III B, the linear behavior of Γ_1 is recovered over the full range of q^2, demonstrating the feasibility of this correction. The solid line in Fig. 4 is a linear fit ($\Gamma_1=Dq^2+C$) of the data corrected for both dark noise and stray light. The fitting parameters are $D=(1.729\pm0.001)\times10^{-9}$ cm^2 s^{-1} and $C=(-1.48\pm1.66)\times10^{-4}$ s^{-1}, indicating that, within the experimental uncertainties, the data exhibit a linear behavior, going through the origin. By means of the Stokes-Einstein relationship $D=k_BT/6\pi\eta R$, we can calculate the particle radius R from the fitted value of D (the viscosity η was measured to be 1.086 ± 0.007 cp at 22 °C). We find $R=1.15\pm0.01\,\mu$m, in good agreement with the manufacturer value, $R=1.095\,\mu$m, obtained with a traditional DLS setup, and for which an estimated error of 0.05 μm was reported.

The effect of the stray light can be appreciated better by plotting the particle radius R, calculated from $D=\Gamma_1/q^2$ and the Stokes–Einstein relationship, as a function of q, shown in Fig. 5. The data corrected only for the dark noise (open circles) show a large increase in R at the smaller angles, due to the underestimation of Γ_1 discussed above. The fully corrected data (filled squares) exhibit considerably less deviation. We emphasize that the correction procedure is effective even for the innermost sets of pixels, for which the stray light intensity is several times larger than the scattering from the sample (see Table I). The large error bars at very low q reflect the inherently poorer statistics of the autocorrelation

functions at the smaller angles, discussed above in connection with Fig. 3(b). In Fig. 5 we also show the value of the particle radius obtained by measuring the autocorrelation functions at much higher angles with a traditional goniometer and hardware correlator. The stars refer to data taken between 18° and 60° and averaged over four runs. As can be seen, there is good agreement between the experimental value of R obtained with the two different techniques and with the value reported by the manufacturer (straight line in Fig. 5), the CCD data being slightly closer to the manufacturer's radius.

In conclusion, we have implemented a setup for measuring DLS at ultralow angles, and we have analyzed the peculiarities and the limitations inherent in the use of a CCD sensor as a detector. The main difficulties are imposed by the reduced dynamic range of the CCD camera, compared to that of the photomultiplier tubes traditionally used for DLS, and by the unavoidable stray light scattered by the optical components of the setup. We have developed a method for correcting the experimental data for the distortions induced by the CCD dark noise, the stray light, and the finite pixel size, that allows us to extract the field autocorrelation function. This feature is of particular interest when the shape of the correlation function is not known *a priori*, or when relevant information are embedded in the presence and the height of a plateau at large time delays, as, for example, is the case for gels. The algorithm and the data correction procedure described here are essential in order to fully exploit the potential of small-angle DLS. More generally, we believe that they will be valuable in all applications were a CCD sensor is used to measure the time autocorrelation of the scattered radiation, an experimental technique of growing interest and importance.

ACKNOWLEDGMENTS

The authors thanks P. Pusey and P. Kaplan for useful discussions, and V. Trappe for carefully reading the manuscript. This work was supported by NASA Grant No. NAG3-2058.

[1] See, for example, B. J. Berne and R. Pecora, *Dynamic Light Scattering* (Wiley, New York, 1976).
[2] See, for example, J. W. Goodman, in *Laser Speckles and Related Phenomena*, edited by J. C. Dainty (Springer, Berlin, 1975).
[3] A. P. Y. Wong and P. Wiltzius, Rev. Sci. Instrum. **64**, 2547 (1993).
[4] S. Kirsch, V. Frenz, W. Schärtl, E. Bartsch, and H. Sillescu, J. Chem. Phys. **104**, 1758 (1996); E. Bartsch, V. Frenz, S. Kirsh, W. Schärtl, and H. Sillescu, Prog. Colloid Polym. Sci. **104**, 40 (1997).
[5] S. B. Dierker, R. Pindak, R. M. Fleming, I. K. Robinson, and L. Berman, Phys. Rev. Lett. **75**, 449 (1995).
[6] S. G. J. Mochrie *et al.*, Phys. Rev. Lett. **78**, 1275 (1997).
[7] O. K. C. Tsui and S. G. J. Mochrie, Phys. Rev. E **57**, 2030 (1998).
[8] F. Ferri, Rev. Sci. Instrum. **68**, 2265 (1997).
[9] K. Schätzel, in *Dynamic Light Scattering. The Method and Some Applications*, edited by W. Brown (Clarendon, Oxford, 1993).
[10] P. N. Pusey and W. Van Megen, Physica A **157**, 705 (1989).
[11] J. G. H. Joosten, E. T. F. Geladé, and P. N. Pusey, Phys. Rev. A **42**, 2161 (1990).
[12] J. Müller and T. Palberg, Prog. Colloid Polym. Sci. **100**, 121 (1996).
[13] J. Z. Xue, D. J. Pine, S. T. Milner, X. L. Wu, and P. M. Chaikin, Phys. Rev. A **46**, 6550 (1992).
[14] See, for example E. Jakemen, in *Photon Correlation and Light Beating Spectroscopy*, edited by H. Z. Cummins and E. R. Pike (Plenum, New York, 1974).
[15] L. Cipelletti, M. Carpineti, and M. Giglio, Phys. Rev. E **57**, 3485 (1998).